Bulletin of Computational Intelligence
https://www.sciltp.com/journals/bci

Article

Endpoint-Controlled Two-Term Asymptotics for Nonlinear Caputo Relaxation: Memory–Constitutive Competition and Hitting Times

Grienggrai Rajchakit

Program in Industrial Optimisation and Applications, Faculty of Science, Maejo University, Chiang Mai 50290, Thailand; kreangkri@mju.ac.th

How To Cite: Rajchakit, G. Endpoint-Controlled Two-Term Asymptotics for Nonlinear Caputo Relaxation: Memory–Constitutive Competition and Hitting Times. *Bulletin of Computational Intelligence* **2026**, *2*(3), 252–272. https://doi.org/10.53941/bci.2026.100014

Received: 4 August 2026
Revised: 13 August 2026
Accepted: 26 August 2026
Published: 31 Aughust 2026

Abstract: We derive two-term asymptotic expansions for nonlinear Caputo relaxation while isolating the recent-history concentration that first-order regular variation does not control. Under a terminal uniform-integrability condition, the Caputo dissipation retains its finite-initial-value term and has an explicit memory correction. Ultimate convexity and a local derivative bound are sufficient for this condition, whereas a plateau–catch-up construction proves that bare regular variation is insufficient. For a restoring law $\phi(x) = cx^\beta\{1 + ax^\sigma + o(x^\sigma)\}$, the state satisfies $u(t) \sim Kt^{-\alpha/\beta}$. Its first relative correction has order $t^{-\alpha\sigma/\beta}$ when $\sigma < 1$ and order $t^{-\alpha/\beta}$ when $\sigma \geq 1$, separating constitutive dominance, resonance, and memory dominance. For the exact-power law, the coefficient changes sign at $\alpha = \beta/(\beta + 1)$; the same sign determines whether the corrected residual hitting time is earlier or later than its leading estimate. At $T = 3000$, implicit L1 diagnostics recover the subcritical and supercritical state coefficients within 0.85% and 4.6%, respectively, and the resonant coefficient within 1%. These computations support the predicted signs and scales but do not replace the analytical endpoint hypothesis.

Keywords: Caputo differential equation; regular variation; nonlinear relaxation; Abelian theorem; asymptotic inversion; hitting time

1. Introduction

The leading tail of scalar Caputo relaxation is now well understood. For

$$^{C}D_t^\alpha u = -\phi(u), \qquad 0 < \alpha < 1,$$

comparison and Volterra methods yield positivity, monotonicity, and power-order decay in broad scalar settings. Feng et al. developed a detailed qualitative theory for one-dimensional autonomous fractional ordinary differential equations [1], while Li and Liu placed such equations in a generalized Caputo and convolution framework [2]. Earlier power-type decay bounds for related weighted Riemann–Liouville Cauchy problems were obtained by Furati and Tatar [3,4], and energy methods give optimal decay orders for wider nonlocal evolution problems [5]. These results establish the relevant scale. A two-sided order estimate, however, neither identifies a normalized limit nor its first relative error.

The distinction is structural. A classical autonomous equation is local in time, whereas the Caputo derivative combines the complete past trajectory with a kernel that becomes unbounded at the current time. The leading dissipation coefficient depends on the total mass lost from the initial state. The next coefficient depends on where the remaining Stieltjes mass is located. Consequently, convergence of $u(tx)/u(t)$ for each fixed $0 < x < 1$ does not control the convolution uniformly as $x \uparrow 1$.

This endpoint obstruction rules out formal differentiation of a regularly varying equivalent. Suppose that $u(t) \sim Kt^{-\rho}$, $0 < \rho < 1$, and write $\nu(ds) = -du(s)$. The Caputo dissipation is a Stieltjes convolution with $(t - s)^{-\alpha}$.

Copyright: © 2026 by the authors. This is an open access article under the terms and conditions of the Creative Commons Attribution (CC BY) license (https://creativecommons.org/licenses/by/4.0/).
Publisher's Note: Scilight stays neutral with regard to jurisdictional claims in published maps and institutional affiliations.

Regular variation controls the rescaled measure on compact subsets of the open interval $0 < s/t < 1$, but the kernel is unbounded as $s/t \uparrow 1$. A small amount of derivative mass compressed next to t can therefore be negligible in the ratio $u(t)/(Kt^{-\rho})$ and still dominate the normalized residual. Classical regular-variation theory supplies the compact convergence, Potter estimates, and monotone-density principles needed away from the endpoint [6], while additional control must be imposed or proved at the singular boundary.

The operator theorem separates two inputs. The state belongs only to $RV_{-\rho}$; no de Haan auxiliary function is assumed. A terminal uniform-integrability condition controls $-du$ on shrinking multiplicative neighborhoods of the observation time. It is stronger than tail regular variation but weaker than a pointwise derivative asymptotic. Section 4 gives two usable sufficient conditions and a counterexample showing why additional terminal control is necessary for a theorem over the entire $RV_{-\rho}$ class.

The result complements, rather than replaces, general fractional regular-variation theory. Řehák studied fractional integration and differentiation of asymptotic relations and developed fractional analogues of Karamata and monotone-density results [7,8]. Second-order regular variation and its transfer through transforms also have an established theory [9,10]. Accordingly, the gamma quotient appearing below is not new in isolation. The present theorem concerns a finite-mass, negative-index Caputo tail: it retains the initial-value term, states the terminal concentration condition explicitly, and pairs the coefficient with a sharpness construction. The nonlinear contribution is the conditional inversion of that operator coefficient against a competing constitutive perturbation.

The theorem-level boundary is as follows.

- Řehák [7,8]: fractional differentiation and integration under regular variation, with established gamma-quotient transfer, but not the finite-mass Caputo decomposition with the explicit terminal test and its failure example.
- de Haan and Stadtmüller [9]; Mao and Hua [10]: second-order regular-variation and transform transfer when an auxiliary rate is supplied. No such second-order auxiliary function is assumed here.
- Theorem 1 and Section 4.3: a decreasing finite-mass $RV_{-\rho}$ trajectory, with an initial-value leading term, signed correction, two sufficient endpoint criteria, and a counterexample under bare $RV_{-\rho}$.
- Theorem 3: conditional nonlinear competition between the memory and constitutive scales under the trajectory hypotheses and (5).

Thus the beta–gamma coefficient is classical; the claimed package is the finite-mass endpoint criterion, the sharpness construction, and its conditional nonlinear inversion.

For the nonlinear application, assume

$$\phi(x) = cx^{\beta}\{1 + ax^{\sigma} + o(x^{\sigma})\}, \qquad x \downarrow 0,$$

with $c > 0$, $\beta > 1$, and $\sigma > 0$, and suppose the trajectory satisfies the stated global and endpoint hypotheses. The leading exponent is $\rho = \alpha/\beta$. The Caputo memory correction has relative order $t^{-\rho}$, whereas the local perturbation in ϕ has relative order $t^{-\rho\sigma}$. Thus the first correction is constitutive for $\sigma < 1$, resonant for $\sigma = 1$, and memory-driven for $\sigma > 1$. For a trajectory of the exact-power equation satisfying the endpoint condition, the memory coefficient contains $\Gamma(1 - \alpha - \rho)^{-1}$. Its sign changes when $\alpha + \rho$ crosses one. At equality, the normalized operator residual vanishes directly. The available hypotheses do not determine a subsequent power.

The proof has four steps. An exact Stieltjes decomposition isolates the finite initial mass. A three-region limit treats the lower endpoint, compact interior, and singular terminal layer separately. A scalar inversion lemma then compares $t^{-\rho}$ with $t^{-\rho\sigma}$ before expanding. The state correction finally transfers to residual hitting times. This order of argument prevents an endpoint assumption, a constitutive expansion, or a formal gamma identity from doing work it cannot justify.

The nonlinear theorem is conditional. Positivity, decrease to zero, and endpoint regularity are assumptions on the trajectory, not consequences of the local expansion of ϕ. Standard scalar theory supports the first two properties under suitable global conditions, but automatic endpoint regularity for every trajectory of the exact-power equation is not proved here. The numerical section cannot replace that implication. Systems, distributed order, delay, and partial differential equations are outside the stated result.

Section 2 fixes the notation and derives the exact decomposition. Section 3 proves the endpoint-regular Abelian theorem, including its critical form. Section 4 gives sufficient criteria and the counterexample. Sections 5 and 6 derive the nonlinear and hitting-time expansions. Sections 7 and 8 present the L1 method and diagnostic calculations. Section 9 compares the result with adjacent theory and records its limitations, and Section 10 states the conclusions. Figure 1 summarizes the logical dependence among the main results and the role of each auxiliary statement.

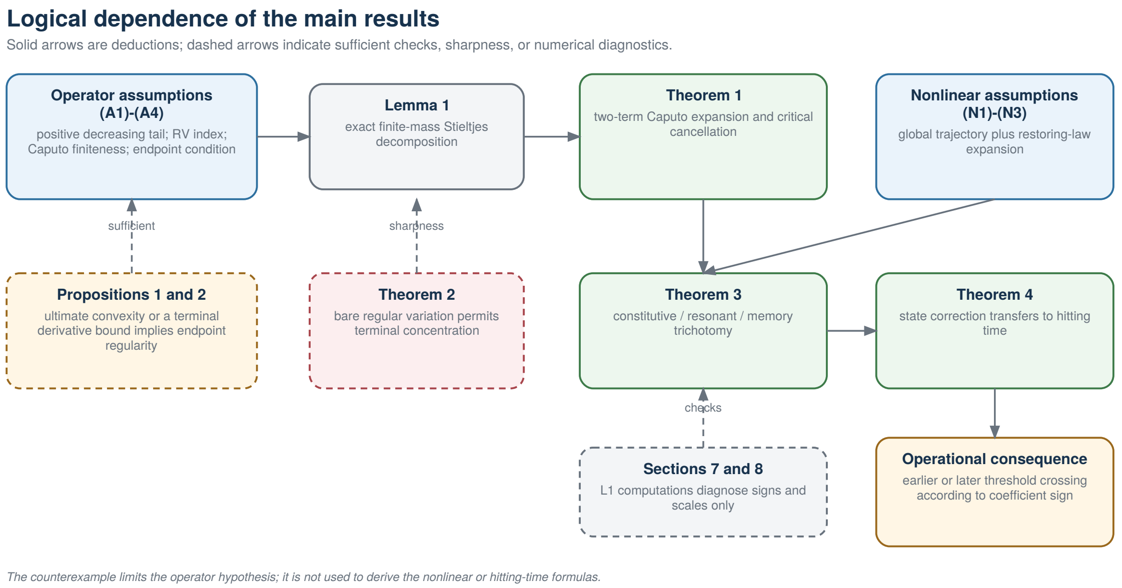

Figure 1. Logical dependence among the main results. Solid arrows denote deductions. Dashed arrows distinguish sufficient endpoint checks, the sharpness construction, and numerical diagnostics from the theorem chain.

2. Preliminaries and Exact Decompositions

2.1. Caputo Derivative and Stieltjes Dissipation

Let $0 < \alpha < 1$. We use the standard Caputo convention described, for example, by Diethelm [11]. For a locally absolutely continuous function u, set

$$^{C}D_t^{\alpha}u(t) = \frac{1}{\Gamma(1-\alpha)} \int_0^t (t-s)^{-\alpha} u'(s)\, ds.$$

The integral is understood at those $t > 0$ for which it is finite. To make the pointwise statements below unambiguous, throughout Sections 2–4 we assume that $u : [0, \infty) \to (0, \infty)$ is locally absolutely continuous, nonincreasing, tends to zero, and satisfies

$$\int_0^t (t-s)^{-\alpha} |u'(s)|\, ds < \infty \quad \text{for every } t > 0. \tag{1}$$

This weighted local condition is automatic, for example, if u' is locally bounded away from the origin. It is separate from the large-time endpoint condition introduced in Section 2.3. Set

$$u_0 = u(0), \qquad \nu(ds) = -du(s).$$

Then ν is a positive Stieltjes measure with total mass $\nu([0, \infty)) = u_0$, and

$$q(t) := -^{C}D_t^{\alpha}u(t) = \frac{1}{\Gamma(1-\alpha)} \int_{[0,t)} (t-s)^{-\alpha} \nu(ds).$$

The half-open endpoint convention is immaterial for locally absolutely continuous u, but it keeps the singular kernel and the measure-theoretic formula compatible.

Local absolute continuity supplies three facts used later. The measure ν has no atoms, so changing an interval endpoint does not alter a displayed integral. Its tail mass is

$$\nu((t, \infty)) = u(t).$$

Integration by parts against s is also legitimate on compact intervals. None of these facts supplies a pointwise asymptotic for $-u'$. That stronger conclusion requires a monotone-density hypothesis and is invoked only in Proposition 1.

A positive function belongs to $RV_{-\rho}$ if

https://doi.org/10.53941/bci.2026.100014

$$\frac{u(tx)}{u(t)} \longrightarrow x^{-\rho} \quad (t \to \infty)$$

for every $x > 0$. We require $0 < \rho < 1$. The upper bound excludes a nonintegrable lower-end contribution in the scaled kernel calculation and also holds in the nonlinear application, where $\rho = \alpha/\beta < 1$. Uniform convergence on compact multiplicative intervals and Potter bounds will be used in their standard forms [6].

2.2. Exact Memory Decomposition

The initial datum can be separated without approximation.

Lemma 1 (exact decomposition). *Under the preceding pointwise Caputo condition, for every $t > 0$,*

$$\begin{aligned}\Gamma(1-\alpha)q(t) - u_0 t^{-\alpha} = &-u(t)t^{-\alpha} \\ &+ \int_{[0,t)} \left[(t-s)^{-\alpha} - t^{-\alpha}\right] \nu(ds).\end{aligned} \tag{2}$$

Proof. Since $\nu([0,t)) = u_0 - u(t)$,

$$\begin{aligned}\Gamma(1-\alpha)q(t) &= t^{-\alpha}\nu([0,t)) \\ &\quad + \int_{[0,t)} \left[(t-s)^{-\alpha} - t^{-\alpha}\right] \nu(ds) \\ &= u_0 t^{-\alpha} - u(t)t^{-\alpha} + \int_{[0,t)} \left[(t-s)^{-\alpha} - t^{-\alpha}\right] \nu(ds).\end{aligned}$$

Rearrangement gives (2). □

Introduce

$$H(x) = (1-x)^{-\alpha} - 1, \qquad 0 \le x < 1,$$

For a Borel set $B \subset [0,\infty)$, write $tB = \{tx : x \in B\}$. With $q(t)$, u_0, and ν defined in (2), define the scaled measure

$$\mu_t(B) = \frac{\nu(tB)}{u(t)}.$$

Multiplying (2) by $t^{\alpha}/u(t)$ gives

$$\frac{t^{\alpha}}{u(t)}\{\Gamma(1-\alpha)q(t) - u_0 t^{-\alpha}\} = -1 + \int_{[0,1)} H(x)\,\mu_t(dx). \tag{3}$$

The measure tails satisfy

$$\mu_t((x,\infty)) = \frac{\nu((tx,\infty))}{u(t)} = \frac{u(tx)}{u(t)} \longrightarrow x^{-\rho}. \tag{4}$$

Hence μ_t converges vaguely on compact subsets of $(0,\infty)$ to the measure $\rho x^{-\rho-1}\,dx$. Formula (3) would immediately yield the coefficient if H were compactly supported and bounded. It is neither.

Compact vague convergence can be read directly from the tails. If $0 < a < b < \infty$, then

$$\mu_t((a,b]) = \frac{u(ta) - u(tb)}{u(t)} \longrightarrow a^{-\rho} - b^{-\rho}.$$

Finite linear combinations of interval indicators therefore converge, and uniform approximation extends the limit to continuous test functions supported inside $(0,\infty)$. This argument does not approach either zero or the singular point one. The endpoint estimates in Theorem 1 provide information that vague convergence does not contain.

2.3. Endpoint Regularity

The lower endpoint is mild because $H(x) = \alpha x + O(x^2)$ as $x \downarrow 0$. The terminal endpoint is singular. We impose

$$\lim_{\delta\downarrow 0}\limsup_{t\to\infty} \frac{t^{\alpha}}{u(t)} \int_{((1-\delta)t,t)} (t-s)^{-\alpha}\nu(ds) = 0. \tag{5}$$

The normalization is dimensionless. The condition states that a terminal multiplicative interval carries asymptotically negligible mass after it is weighted by the unbounded Caputo kernel.

An intuitive reading is that the most recent fraction of the trajectory must not contain a hidden burst of dissipation. A small state drop is harmless when it is spread over a macroscopic interval. The same drop can be strongly amplified if it is released immediately before the observation time, because the Caputo weight $(t-s)^{-\alpha}$ then becomes large. Condition (5) excludes such terminal concentration only after the natural normalization by the tail size $u(t)$. In physical terms, it rules out an increasingly impulsive last-moment release of stored state while allowing ordinary smooth or mildly oscillatory relaxation.

The order of limits is part of the definition. For fixed δ, the observation time tends to infinity first. Only then is the terminal fraction reduced. Reversing these operations would make the interval empty at every fixed time and would test nothing. A constant used in the terminal estimate must be independent of t and of the later choice of δ. Otherwise the final limit cannot be taken.

Condition (5) is used only for $s/t \uparrow 1$. It is stronger than ordinary regular variation, but Section 4 shows that it follows from natural derivative bounds. Section 4 also constructs a regularly varying decreasing function for which the condition fails. The theorem therefore keeps separate the information supplied by the tail ratio (4) and the uniform integrability required by the singular kernel.

2.4. The Beta–Gamma Constant

The limiting coefficient can be evaluated without separating divergent integrals. For $0 < \alpha, \rho < 1$, define

$$F(z) = \int_0^1 \big[(1-x)^{-\alpha} - 1\big] x^{z-1}\, dx.$$

The integral is analytic for $\Re z > -1$. For $\Re z > 0$,

$$F(z) = B(z, 1-\alpha) - \frac{1}{z},$$

and analytic continuation to $z = -\rho$ yields

$$\rho F(-\rho) - 1 = -\frac{\Gamma(1-\rho)\Gamma(1-\alpha)}{\Gamma(1-\alpha-\rho)}. \tag{6}$$

Whenever the denominator reaches a pole, the quotient is interpreted through the entire reciprocal-gamma function $1/\Gamma$. In particular, $1/\Gamma(0) = 0$. The direct argument below verifies the same critical value without relying on this convention. At the critical relation $\alpha + \rho = 1$, the zero can also be verified directly. Since

$$\rho\big[(1-x)^{\rho-1} - 1\big] x^{-\rho-1} = \frac{d}{dx}\left\{ x^{-\rho} - \left(\frac{1-x}{x}\right)^{\rho} \right\},$$

integration from zero to one gives

$$\rho \int_0^1 \big[(1-x)^{\rho-1} - 1\big] x^{-\rho-1}\, dx = 1. \tag{7}$$

Thus the normalized residual in (3) has limit zero at the threshold for a reason visible in the integral itself.

3. Endpoint-Regular Second-Order Caputo Asymptotics

3.1. Compact-Interior Convergence

We first isolate the only place where terminal control is needed.

For clarity, the operator theorem uses the following assumption ledger.

Assumption A1. $0 < \alpha < 1$ *and* $0 < \rho < 1$.

Assumption A2. $u : [0, \infty) \to (0, \infty)$ *is locally absolutely continuous, nonincreasing, and tends to zero.*

Assumption A3. $u \in RV_{-\rho}$ *and satisfies the pointwise Caputo integrability condition (1).*

Assumption A4. *The terminal uniform-integrability condition (5) holds.*

Theorem 1 (endpoint-regular Abelian expansion)**.** *Hypotheses. Assumptions (A1)–(A4). Conclusion.*

$$q(t) = \frac{u_0}{\Gamma(1-\alpha)} t^{-\alpha} - \frac{\Gamma(1-\rho)}{\Gamma(1-\alpha-\rho)} u(t)t^{-\alpha} + o\big(u(t)t^{-\alpha}\big)\,. \tag{8}$$

If $\alpha+\rho=1$, the second displayed coefficient vanishes and

$$q(t) - \frac{u_0}{\Gamma(1-\alpha)} t^{-\alpha} = o\big(u(t)t^{-\alpha}\big)\,. \tag{9}$$

Proof. It suffices, by (3), to prove

$$\int_{[0,1)} H(x)\,\mu_t(dx) \longrightarrow \rho \int_0^1 H(x)x^{-\rho-1}\,dx. \tag{10}$$

Fix $0<\varepsilon<1-\delta<1$. On $[\varepsilon,1-\delta]$, the function H is continuous and bounded. The tail convergence (4) implies vague convergence of μ_t, hence

$$\int_{[\varepsilon,1-\delta]} H\,d\mu_t \longrightarrow \rho \int_\varepsilon^{1-\delta} H(x)x^{-\rho-1}\,dx. \tag{11}$$

We next show that the two discarded regions can be made uniformly small.

Choose a fixed $T>0$. When $t>2T$, the estimate $H(s/t)\le C_\alpha s/t$ holds for $0\le s\le T$. Therefore

$$\int_{[0,T/t]} H\,d\mu_t \le \frac{C_\alpha}{t\,u(t)} \int_{[0,T]} s\,\nu(ds). \tag{12}$$

The numerator is fixed. Since $u(t)=t^{-\rho}L(t)$ for a slowly varying L and $\rho<1$, $t\,u(t)\to\infty$, so the right-hand side tends to zero.

For the remaining lower interval, use

$$\int_{(0,y]} s\,\nu(ds) = \int_0^y u(s)\,ds - yu(y). \tag{13}$$

Karamata's integral theorem gives

$$\int_0^y u(s)\,ds - yu(y) \sim \frac{\rho}{1-\rho} yu(y). \tag{14}$$

Let $\eta\in(0,1-\rho)$ and fix $\varepsilon_0\in(0,1/2)$. Potter's bound may be chosen uniformly for $0<\varepsilon\le\varepsilon_0$ once T and ε_0 are fixed. Combining it with (12)–(14) gives constants C, C', independent of the later choice of ε, such that for all sufficiently large t,

$$\int_{(T/t,\varepsilon]} H\,d\mu_t \le C\frac{\varepsilon t\,u(\varepsilon t)}{t\,u(t)} \le C'\varepsilon^{1-\rho-\eta}. \tag{15}$$

The exponent is positive, so this bound vanishes with ε. The same estimates apply to the limiting integral near zero because $H(x)x^{-\rho-1}=O(x^{-\rho})$.

For the terminal interval, $0\le H(s/t)\le t^\alpha(t-s)^{-\alpha}$. Consequently,

$$\int_{(1-\delta,1)} H\,d\mu_t \le \frac{t^\alpha}{u(t)} \int_{((1-\delta)t,t)} (t-s)^{-\alpha}\nu(ds). \tag{16}$$

Condition (5) sends the iterated limsup of (16) to zero as $\delta\downarrow 0$. The limiting density has the same property because $(1-x)^{-\alpha}$ is integrable at one.

Taking $t\to\infty$ in (11), then $\varepsilon\downarrow 0$ and $\delta\downarrow 0$, proves (10). Equations (3) and (6) now give

$$\frac{t^\alpha}{u(t)}\{\Gamma(1-\alpha)q(t) - u_0t^{-\alpha}\} \longrightarrow -\frac{\Gamma(1-\rho)\Gamma(1-\alpha)}{\Gamma(1-\alpha-\rho)}.$$

Division by $\Gamma(1-\alpha)$ gives (8). At $\alpha+\rho=1$, identity (7) makes the limit zero before the gamma notation is invoked, which proves (9). □

For later reuse, the convergence argument admits an explicit error ledger. Let

$$R(t) = -1 + \int_{[0,1)} H(x)\,\mu_t(dx), \qquad G = -1 + \rho \int_0^1 H(x)x^{-\rho-1}\,dx.$$

For every $0 < \varepsilon < 1 - \delta < 1$, the triangle inequality gives

$$\begin{aligned} |R(t) - G| \le & \left| \int_{[\varepsilon,1-\delta]} H\,d\mu_t - \rho \int_\varepsilon^{1-\delta} H(x)x^{-\rho-1}\,dx \right| \\ & + \int_{[0,\varepsilon)} H\,d\mu_t + \int_{(1-\delta,1)} H\,d\mu_t \\ & + \rho \int_0^\varepsilon H(x)x^{-\rho-1}\,dx + \rho \int_{1-\delta}^1 H(x)x^{-\rho-1}\,dx. \end{aligned} \tag{17}$$

The first term tends to zero for fixed ε, δ by (11); the second is controlled by (12)–(15); the third is controlled by (5); and the last two are integrable endpoint tails. Thus (17) records the order of limits without asserting a convergence rate not supplied by the hypotheses. It also identifies the four independent quantities that a quantitative refinement would have to estimate.

The proof uses every hypothesis in a localized way. Positivity and decrease turn $-du$ into a finite positive measure. The limit $u(t) \to 0$ identifies its total mass as u_0. Regular variation gives (4), the lower-end Karamata estimate, and the compact-interior limit. The restriction $\rho < 1$ makes the lower limiting integrand integrable. Endpoint regularity appears only in (16), while local absolute continuity removes atoms and permits (13). Weakening one assumption should therefore change the corresponding proof region rather than being hidden in a global smoothness phrase.

The limit order can be written as an epsilon argument. Given $\zeta > 0$, first choose ε so that the lower bounds in (15) and their limiting analogues are below ζ. Next choose δ so that the endpoint limsup and the limiting terminal integral are below ζ. With both values fixed, choose t large enough for the compact convergence (11) and fixed-interval estimate (12). The total error is then bounded by a constant multiple of ζ. Sending $\zeta \downarrow 0$ proves (10) without exchanging uncontrolled limits.

3.2. Sign and Scale

The second coefficient reflects a genuine sign boundary. If $\alpha + \rho < 1$, then $\Gamma(1 - \alpha - \rho) > 0$, and the correction in (8) is negative. If $1 < \alpha + \rho < 2$, then $-1 < 1 - \alpha - \rho < 0$, so $\Gamma(1 - \alpha - \rho) < 0$, and the correction is positive. At equality, the term cancels.

The critical scale must retain any slowly varying factor. For a general $u(t) = t^{-\rho}L(t)$, (9) is

$$q(t) - \frac{u_0}{\Gamma(1-\alpha)} t^{-\alpha} = o(t^{-1}L(t)).$$

Only after the nonlinear model gives $u(t) \sim Kt^{-\rho}$ can this be written as $o(t^{-1})$. This distinction prevents a slowly varying term from being discarded without proof.

Theorem 1 complements rather than replaces fractional regular-variation results. The operator literature supplies broad Abelian and Tauberian principles [7,8]. Here the finite initial value creates a dominant $u_0 t^{-\alpha}$ term, and the next coefficient depends on controlling an unbounded terminal kernel. The next section tests the hypothesis from both sides.

A smooth power tail provides a useful consistency test. For $u(t) = (1 + t)^{-\rho}$, the trajectory is decreasing and convex, so Proposition 1 applies. The normalized residual in (3) then converges to the constant in (6). This calculation checks the scale and sign but cannot establish the theorem, because it excludes the terminal-concentration mechanism by construction.

4. Sufficient Conditions and Sharpness

4.1. Ultimate Convexity

Condition (5) is not verifiable from the tail of u alone, so a structural sufficient condition is needed. Ultimate convexity is the most convenient one in practice, because it converts regular variation of the state into a pointwise asymptotic for the derivative and thereby bounds the terminal derivative mass directly.

Proposition 1. *Under the hypotheses of Theorem 1 except (5), assume in addition that u is ultimately convex. Then (5) holds.*

Proof. On the ultimately convex tail, let f be the nonincreasing right-derivative representative of $-u'$; it agrees with $-u'$ almost everywhere. Since

$$u(t) = \int_t^\infty f(s)\,ds$$

and $u \in RV_{-\rho}$, the monotone-density theorem gives

$$f(t) \sim \rho\frac{u(t)}{t}. \tag{18}$$

Fix $\delta_0 \in (0, 1/2)$. Uniform convergence of regularly varying functions and (18) give a constant C such that

$$f(s) \le C\frac{u(t)}{t} \quad \text{whenever} \quad s \in [(1-\delta_0)t, t] \tag{19}$$

and t is sufficiently large. For $0 < \delta \le \delta_0$,

$$\begin{aligned}\int_{(1-\delta)t}^{t}(t-s)^{-\alpha}\nu(ds) &= \int_{(1-\delta)t}^{t}(t-s)^{-\alpha}f(s)\,ds \\ &\le \frac{Cu(t)}{t}\frac{(\delta t)^{1-\alpha}}{1-\alpha} \\ &= \frac{C}{1-\alpha}u(t)t^{-\alpha}\delta^{1-\alpha}.\end{aligned}$$

Multiplication by $t^\alpha/u(t)$, followed by $\delta \downarrow 0$, proves the claim. □

Ultimate convexity is sufficient, not automatic. Feng et al. used convexity as a hypothesis in the relevant numerical analysis [1]. That result does not establish ultimate convexity for every nonlinear power trajectory. The main theorem therefore retains endpoint regularity explicitly.

The estimate is stable under finite modifications of the trajectory. Convexity and the derivative asymptotic are needed only after a sufficiently large time. Any initial interval contributes through (12), where its fixed first moment is divided by $t\,u(t) \to \infty$. Thus the sufficient condition can be checked on the asymptotic tail even when a Caputo solution has a weak derivative singularity near the initial time.

4.2. Direct Derivative Control

The proof above uses only a local bound, not the full convexity statement.

Proposition 2. *Under the hypotheses of Theorem 1 except (5), suppose that there exist $C > 0$ and $\delta_0 \in (0, 1)$ such that*

$$\operatorname*{ess\,sup}_{s\in[(1-\delta_0)t,t]} \frac{t[-u'(s)]}{u(t)} \le C \tag{20}$$

for all sufficiently large t. Then (5) holds.

Proof. Replace (19) by (20) and repeat the last integral estimate in the proof of Proposition 1. □

Smooth variation with $-tu'(t)/u(t) \to \rho$, together with local uniform domination, implies (20). The domination clause matters. A derivative equivalence is not a consequence of $u(t) \sim Kt^{-\rho}$ alone.

The converse implication is neither assumed nor needed. Condition (5) controls a weighted terminal average and can hold even when $-u'$ has local oscillations. Proposition 2 is a transparent pointwise route to the integral condition, not an alternative definition of the admissible class.

4.3. Plateau–Catch-Up Counterexample

The terminal condition cannot be replaced by ordinary regular variation.

Before the technical construction, Figure 2 summarizes the mechanism. On a shrinking window, replace a smooth descent by a long plateau followed by a much shorter affine catch-up. The maximum relative height error is only $O(\ell_n)$, so the function remains asymptotic to the smooth power tail. The delayed Stieltjes mass is nevertheless released at distance $O(\delta_n T_n)$ from the terminal time. The singular kernel amplifies that compressed mass by $\delta_n^{-\alpha}$.

Theorem 2 (concentration counterexample)**.** *For every $0 < \alpha < 1$ and $0 < \rho < 1$, there exists a positive, nonincreasing, locally absolutely continuous function $u \in RV_{-\rho}$ such that (5) fails and*

$$\frac{t^{\alpha}}{u(t)}\{\Gamma(1-\alpha)q(t) - u_0 t^{-\alpha}\}$$

is unbounded along a sequence.

Proof. Let $v(t) = (1+t)^{-\rho}$. Choose $T_n \uparrow \infty$ so rapidly that the intervals

$$I_n = [(1-\ell_n)T_n, T_n]$$

are disjoint, where $\ell_n \downarrow 0$. Put $\delta_n = \ell_n^{2/\alpha}$. For all sufficiently large n, $0 < \delta_n < \ell_n$. Define

$$a_n = (1-\ell_n)T_n, \qquad b_n = (1-\delta_n)T_n.$$

For example, fix $\ell_n = 2^{-n}$ and choose T_{n+1} recursively so that

$$(1-\ell_{n+1})T_{n+1} > 2T_n.$$

The modified windows are then disjoint, and every compact interval meets only finitely many pieces. Outside the union of the I_n, set $u = v$. On $[a_n, b_n]$, set

$$u(t) = v(a_n).$$

On $[b_n, T_n]$, let u be the affine function joining $(b_n, v(a_n))$ to $(T_n, v(T_n))$.

The pieces match at every endpoint, so u is continuous and locally absolutely continuous. It is positive and nonincreasing. The base function v is convex. Its chord from b_n to T_n lies above its graph, and raising the left endpoint from $v(b_n)$ to $v(a_n)$ preserves that inequality. Hence $u(t) \geq v(t)$ throughout each modified window. Also,

$$1 \leq \frac{u(t)}{v(t)} \leq \frac{v(a_n)}{v(T_n)} = \left(1 - \ell_n \frac{T_n}{1+T_n}\right)^{-\rho} = 1 + O(\ell_n) \longrightarrow 1$$

uniformly on I_n. Outside the windows the ratio is one. Thus $u(t)/v(t) \to 1$, and $u \in RV_{-\rho}$.

Uniform equivalence proves the last claim even when t and tx lie in different windows. For each fixed $x > 0$,

$$\frac{u(tx)}{u(t)} = \frac{u(tx)}{v(tx)}\frac{v(tx)}{v(t)}\frac{v(t)}{u(t)} \longrightarrow x^{-\rho}.$$

Both outer ratios converge globally to one, while the middle ratio is regularly varying.

The catch-up interval carries Stieltjes mass

$$m_n = v(a_n) - v(T_n) \sim \rho \ell_n v(T_n). \tag{21}$$

This mass is distributed uniformly over an interval of length $\delta_n T_n$. At $t = T_n$, its contribution to the endpoint integral is

$$\begin{aligned}\int_{[b_n,T_n)} (T_n - s)^{-\alpha}\nu(ds) &= \frac{m_n}{\delta_n T_n}\int_0^{\delta_n T_n} r^{-\alpha}\,dr \\ &= \frac{m_n}{1-\alpha}(\delta_n T_n)^{-\alpha}.\end{aligned}$$

After normalization,

$$\frac{T_n^{\alpha}}{u(T_n)}\int_{[b_n,T_n)} (T_n - s)^{-\alpha}\nu(ds) \sim \frac{\rho}{1-\alpha}\ell_n \delta_n^{-\alpha} = \frac{\rho}{1-\alpha}\ell_n^{-1} \to \infty. \tag{22}$$

Thus (5) fails. More precisely, the contribution of the catch-up interval to the kernel-difference integral in (3) is

$$\begin{aligned}\int_{[b_n/T_n,1)} H\,d\mu_{T_n} &= \frac{T_n^{\alpha}}{u(T_n)}\int_{[b_n,T_n)} (T_n - s)^{-\alpha}\nu(ds) - \frac{m_n}{u(T_n)} \\ &\sim \frac{\rho}{1-\alpha}\ell_n^{-1},\end{aligned} \tag{23}$$

because $m_n/u(T_n) \sim \rho\ell_n$. Finally, the kernel difference in (2) is nonnegative for every $0 \le s < t$, so the divergent contribution in (23) cannot be cancelled by the remaining windows or by the base profile. The normalized residual equals -1 plus this nonnegative integral and is therefore unbounded along T_n. □

For every fixed $\delta > 0$, eventually $\delta_n < \delta$. Hence the fixed terminal window $((1-\delta)T_n, T_n)$ contains the entire catch-up layer, and its inner limsup in (5) is infinite. The construction is piecewise affine on compact intervals with finitely many breakpoints and bounded local slopes; it therefore satisfies the pointwise condition (1).

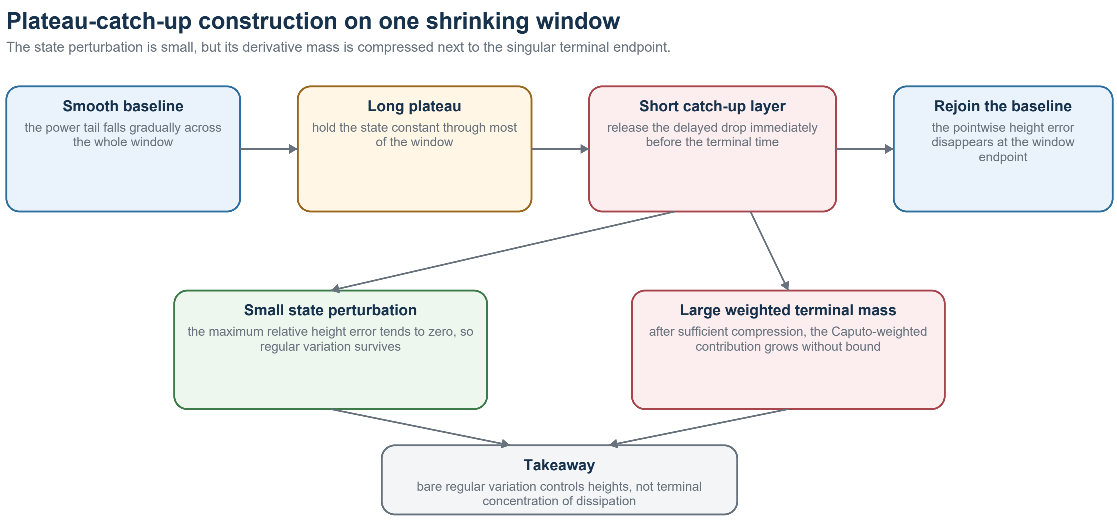

Figure 2. Schematic of one plateau–catch-up window. The construction changes state values by a vanishing relative amount but concentrates the corresponding loss immediately before T_n. With $\delta_n = \ell_n^{2/\alpha}$, the normalized weighted contribution is proportional to $\ell_n\delta_n^{-\alpha} = \ell_n^{-1}$.

The theorem does not claim that the displayed condition is logically necessary in every possible formulation. It proves the needed sharpness statement: bare first-order regular variation does not control a singular terminal convolution. Some endpoint condition or comparably strong local information is indispensable for Theorem 1.

The example is deliberately extremal in how it concentrates derivative mass, so it should not be interpreted as a typical smooth relaxation trajectory. It is not pathological with respect to the theorem's admissible class: it is positive, decreasing, locally absolutely continuous, piecewise affine on each modified window, and regularly varying. Its representative role is narrower and precise. It realizes the only mechanism left uncontrolled by compact regular-variation limits, namely concentration next to the singular endpoint. Smooth trajectories satisfying Proposition 1 or 2 exclude this mechanism.

The construction also shows why oscillating function values alone would not be an adequate counterexample. The Caputo residual integrates derivative mass, so the perturbation must control both the height error and the width of the catch-up. Here the height error is $O(\ell_n)$, while the compressed width $\delta_n T_n$ makes the weighted mass grow as ℓ_n^{-1}. Those conclusions coexist because the kernel is unbounded at the terminal endpoint.

5. Nonlinear Relaxation and Competing Second-Order Mechanisms

5.1. Standing Assumptions and the Leading Law

Return to

$$ {}^{C}D_t^{\alpha}u(t) = -\phi(u(t)), \qquad u(0) = u_0 > 0. \tag{24} $$

The nonlinear application uses three additional assumptions.

Assumption N1. *A global solution is continuous on $[0,\infty)$, locally absolutely continuous on $(0,\infty)$, satisfies (1), and solves (24) for every $t > 0$.*

Assumption N2. *The trajectory is positive, nonincreasing, bounded by u_0, and tends to zero.*

Assumption N3. *The restoring law $\phi : [0, u_0] \to [0,\infty)$ is continuous, strictly increasing near zero, satisfies $\phi(0) = 0$, and has the expansion*

$$\phi(x) = cx^{\beta}\{1 + ax^{\sigma} + r(x)\}, \qquad r(x) = o(x^{\sigma}). \tag{25}$$

Here $c > 0$, $\beta > 1$, $\sigma > 0$, and $a \in \mathbb{R}$. Assumption (N3) is local at zero except for continuity on the compact state interval. This compact state domain is sufficient because the trajectory remains in $[0, u_0]$; no behavior of ϕ outside that interval enters the proof. Positivity and monotonicity for autonomous scalar fractional equations can be obtained under standard structural hypotheses [1]. They are retained as explicit trajectory assumptions rather than inferred from the local expansion (25).

Set $q(t) = \phi(u(t))$. Since u is nonincreasing and ϕ is increasing near zero, q is bounded, locally integrable, and eventually nonincreasing. Condition (1) implies $\int_0^t |u'(s)|\,ds < \infty$ for every $t > 0$, because $(t-s)^{-\alpha} \geq t^{-\alpha}$. Continuity at zero and local absolute continuity on $(0, \infty)$ therefore give $u(t) - u_0 = \int_0^t u'(s)\,ds$. Monotonicity and $u(t) \to 0$ further yield $\int_0^\infty |u'(s)|\,ds = u_0$. Fubini's theorem is consequently applicable to the exponentially weighted Caputo convolution, and (24) gives

$$\widehat{q}(\lambda) = u_0\lambda^{\alpha-1} - \lambda^{\alpha}\widehat{u}(\lambda). \tag{26}$$

Boundedness and $u(t) \to 0$ imply

$$\lambda\widehat{u}(\lambda) = \int_0^\infty e^{-s}u(s/\lambda)\,ds \longrightarrow 0 \quad (\lambda \downarrow 0) \tag{27}$$

by dominated convergence. Hence

$$\widehat{q}(\lambda) \sim u_0\lambda^{\alpha-1}. \tag{28}$$

The monotone-density form of the Karamata–Feller theorem gives

$$q(t) \sim At^{-\alpha}, \qquad A = \frac{u_0}{\Gamma(1-\alpha)}. \tag{29}$$

This exact first-order coefficient refines order bounds without changing the qualitative theory. Its Tauberian mechanism is classical [6].

The inverse of the regularly varying function ϕ now yields

$$u(t) \sim Kt^{-\rho}, \qquad \rho = \frac{\alpha}{\beta}, \qquad K = \left(\frac{A}{c}\right)^{1/\beta} = \left\{\frac{u_0}{c\Gamma(1-\alpha)}\right\}^{1/\beta}. \tag{30}$$

No asymptotic equivalence has been differentiated. The route is transform asymptotics, monotone density for q, and inversion of the restoring law.

The Tauberian hypothesis is visible. Eventual monotonicity of q upgrades the transform equivalence (28) to the pointwise statement (29). Without that hypothesis, the transform would still determine an averaged law, but narrow positive spikes could prevent a pointwise limit. Here monotonicity is inherited from the assumed decrease of u and the increase of ϕ near zero.

Asymptotic inversion uses only the local behavior of ϕ. Since $\phi(x)/(cx^{\beta}) \to 1$, the inverse is regularly varying at zero with index $1/\beta$. Applying it to (29) proves (30). The argument does not require ϕ to be an exact power away from the origin.

5.2. Memory Correction to the Dissipation

Assume in addition that u satisfies (5). Theorem 1 and (30) give

$$\begin{aligned} q(t) &= At^{-\alpha} - \frac{K\Gamma(1-\rho)}{\Gamma(1-\alpha-\rho)}t^{-\alpha-\rho} + o(t^{-\alpha-\rho}) \\ &= At^{-\alpha}\{1 + M_{\alpha,\beta}t^{-\rho} + o(t^{-\rho})\}, \end{aligned} \tag{31}$$

where

$$M_{\alpha,\beta} = -\frac{K\Gamma(1-\alpha)\Gamma(1-\rho)}{u_0\Gamma(1-\alpha-\rho)}. \tag{32}$$

At $\alpha + \rho = 1$, formula (31) means

$$q(t) = At^{-\alpha}\{1 + o(t^{-\rho})\} \tag{33}$$

and $M_{\alpha,\beta} = 0$ records the cancellation. Equation (33), not formal substitution into a pole, is the statement used below.

The sign of $M_{\alpha,\beta}$ is opposite to the sign of $\Gamma(1-\alpha-\rho)$. All other factors in (32) are positive. Thus the memory correction to q is negative below the critical surface and positive above it. The state correction divides this coefficient by β in the exact-power case, so the sign is preserved by nonlinear inversion.

5.3. An Inversion Lemma

The memory and constitutive terms must be compared before any series is expanded.

Lemma 2 (first-correction inversion)**.** *Hypotheses. Let $z(t) \to 1$, $b \in \mathbb{R}$, $\lambda, \mu > 0$, $\beta > 0$, and $\sigma > 0$. Assume*

$$z(t)^\beta \{1 + b\, t^{-\mu} z(t)^\sigma + o(t^{-\mu})\} = 1 + m\, t^{-\lambda} + o(t^{-\lambda}), \tag{34}$$

where the remainder multiplying $t^{-\mu}$ is locally uniform for z near one. Conclusion.

$$z(t) = \begin{cases} 1 - \dfrac{b}{\beta} t^{-\mu} + o(t^{-\mu}), & \mu < \lambda, \\ 1 + \dfrac{m-b}{\beta} t^{-\lambda} + o(t^{-\lambda}), & \mu = \lambda, \\ 1 + \dfrac{m}{\beta} t^{-\lambda} + o(t^{-\lambda}), & \lambda < \mu. \end{cases} \tag{35}$$

Proof. Put $r = \min\{\lambda, \mu\}$. The bracket in (34) is $1 + O(t^{-\mu})$ because $z(t) \to 1$, while the right-hand side is $1 + O(t^{-\lambda})$. Hence $z(t)^\beta = 1 + O(t^{-r})$. The inverse map $x \mapsto x^{1/\beta}$ is locally Lipschitz near one, and therefore $z(t) - 1 = O(t^{-r})$. Write $z = 1 + \eta$. Then

$$z^\beta = 1 + \beta\eta + o(\eta), \qquad z^\sigma = 1 + o(1).$$

If $\mu < \lambda$, division by $t^{-\mu}$ gives $\beta t^\mu \eta + b \to 0$. If $\mu = \lambda$, it gives $\beta t^\lambda \eta + b \to m$. If $\lambda < \mu$, it gives $\beta t^\lambda \eta \to m$. These are the three lines of (35). □

The lemma provides only the first correction. When $0 < \sigma < 1$, repeated powers generated by a longer inverse series may occur before the memory scale $t^{-\rho}$. Formula (25) does not contain the higher constitutive information needed to identify all of them, so no such claim is made.

The local uniformity condition on the remainder is automatic for the application because $z(t) \to 1$ and

$$\frac{r(Kt^{-\rho} z(t))}{(Kt^{-\rho} z(t))^\sigma} \longrightarrow 0.$$

It prevents the $o(x^\sigma)$ term in (25) from changing scale after the normalization.

5.4. Constitutive-Memory Trichotomy

The leading law, the memory correction, and the inversion lemma can now be combined. The next theorem records the resulting first relative correction and shows that its scale and coefficient are decided by the comparison between the memory exponent ρ and the constitutive exponent $\rho\sigma$.

Theorem 3. *Hypotheses. Assume (N1)–(N3) and (5), and let ρ, K, and $M_{\alpha,\beta}$ be given by (30) and (32). Conclusion.*

$$u(t) = Kt^{-\rho} \begin{cases} \left\{1 - \dfrac{aK^\sigma}{\beta} t^{-\rho\sigma} + o(t^{-\rho\sigma})\right\}, & 0 < \sigma < 1, \\ \left\{1 + \dfrac{M_{\alpha,\beta} - aK}{\beta} t^{-\rho} + o(t^{-\rho})\right\}, & \sigma = 1, \\ \left\{1 + \dfrac{M_{\alpha,\beta}}{\beta} t^{-\rho} + o(t^{-\rho})\right\}, & \sigma > 1. \end{cases} \tag{36}$$

Proof. Put

$$u(t) = Kt^{-\rho} z(t).$$

By (30), $z(t) \to 1$. Divide (25), evaluated at $u(t)$, by $At^{-\alpha} = cK^\beta t^{-\rho\beta}$. This gives

$$\frac{q(t)}{At^{-\alpha}} = z(t)^\beta \{1 + aK^\sigma t^{-\rho\sigma} z(t)^\sigma + o(t^{-\rho\sigma})\}. \tag{37}$$

Equation (31) supplies the right-hand side of (34) with

$$m = M_{\alpha,\beta}, \qquad \lambda = \rho, \qquad b = aK^{\sigma}, \qquad \mu = \rho\sigma.$$

Lemma 2 gives the three cases in (36). □

Every hypothesis has a separate use. The global trajectory assumptions make q eventually monotone and justify the transform identity. The expansion of ϕ gives both the leading inverse and the constitutive coefficient. Endpoint regularity supplies (31). The inequality $\beta > 1$ ensures $\rho < 1$, as required in Theorem 1. No convexity assumption is used unless it is chosen as a sufficient route through Proposition 1.

The regimes are determined by exponents. For $0 < \sigma < 1$, the local restoring-law perturbation decays more slowly than the memory correction and therefore controls the first bias. At $\sigma = 1$, both mechanisms occur at the same scale and may reinforce or cancel. For $\sigma > 1$, the constitutive perturbation is smaller and the first correction is universal within the stated endpoint class.

At resonance, the coefficient may cancel for $a = M_{\alpha,\beta}/K$. Such cancellation removes the first displayed term but does not improve the known remainder. A valid next term would require a sharper expansion of both the Caputo operator and ϕ.

This restriction on higher-order claims is substantive, not merely technical. The error ledger (17) proves convergence of the normalized Caputo residual but supplies no rate: (5) is a qualitative uniform-integrability condition, and ordinary regular variation likewise gives no second auxiliary rate. Independently, (25) specifies only an $o(x^{\sigma})$ constitutive remainder. After a resonant or critical cancellation, either unknown remainder can occur before any proposed next power. A third term therefore requires both a rate-strengthened endpoint/operator hypothesis and an explicit next coefficient in the expansion of ϕ. Without those two inputs, assigning a universal exponent would exceed the assumptions.

5.5. Conditional Exact-Power Consequences and Threshold Inversion

Assume now the exact-power law

$$\phi(x) \equiv cx^{\beta},$$

so $a = 0$ and $r \equiv 0$. An exact power satisfies (25) with any chosen $\sigma > 1$; applying the $\sigma > 1$ branch of Theorem 3, conditional on (5), gives

$$u(t) = Kt^{-\rho}\{1 + D_{\alpha,\beta}t^{-\rho} + o(t^{-\rho})\}, \tag{38}$$

where

$$D_{\alpha,\beta} = -\frac{K\Gamma(1-\alpha)\Gamma(1-\rho)}{\beta u_0 \Gamma(1-\alpha-\rho)}. \tag{39}$$

Since $0 < \alpha + \rho < 2$,

$$\operatorname{sgn} D_{\alpha,\beta} = \begin{cases} -1, & \alpha + \rho < 1, \\ 0, & \alpha + \rho = 1, \\ +1, & \alpha + \rho > 1. \end{cases} \tag{40}$$

The threshold is

$$\alpha = \frac{\beta}{\beta + 1}. \tag{41}$$

Below it, the leading profile overestimates the state at first correction. Above it, the leading profile underestimates the state. At the threshold,

$$u(t) = Kt^{-\rho}\{1 + o(t^{-\rho})\}. \tag{42}$$

The remainder in (42) is not assigned a power without a new operator expansion.

Formula (39) also respects the natural scaling of the equation. If $u = u_0 v$ and time is rescaled so that the coefficient of v^{β} is one, then K/u_0 supplies the only amplitude factor in the relative correction. The gamma quotient is dimensionless. This check rules out an extra factor of c, u_0, or $\Gamma(1-\alpha)$ in (39).

5.6. The Unresolved Automatic-Convexity Route

For the exact-power equation, formal differentiation of the Volterra formulation suggests a possible route to endpoint regularity. With $y = -u' > 0$, one obtains

$$y + I^{\alpha}(c\beta u^{\beta-1}y) = \frac{cu_0^{\beta}}{\Gamma(\alpha)}t^{\alpha-1}. \tag{43}$$

Positivity of y does not imply that y decreases. A proof of eventual decrease would require a resolvent or comparison argument compatible with the weak singularity in (43). Classical Volterra theory provides relevant tools [12,13], but those results do not supply the required decrease of y for every parameter pair in (24). Consequently, automatic ultimate convexity remains open here. Theorem 3 is conditional on (5), and Propositions 1 and 2 give two independent routes for verifying that condition on a given trajectory.

6. Corrected Residual Hitting Times

Let

$$T_{\varepsilon} = \inf\{t \geq 0 : u(t) \leq \varepsilon\}.$$

Continuity, nonincrease, and convergence to zero make this generalized inverse finite for every sufficiently small $\varepsilon > 0$. A flat interval does not affect the asymptotic argument. The infimum selects its left endpoint.

Theorem 4. *Hypotheses. Let $u : [0, \infty) \to (0, \infty)$ be continuous and nonincreasing, with $u(t) \to 0$, and assume*

$$u(t) = Kt^{-\rho}\{1 + Dt^{-\lambda} + o(t^{-\lambda})\}, \qquad K, \rho, \lambda > 0. \tag{44}$$

Conclusion. As $\varepsilon \downarrow 0$,

$$T_{\varepsilon} = \left(\frac{K}{\varepsilon}\right)^{1/\rho}\left[1 + \frac{D}{\rho}\left(\frac{\varepsilon}{K}\right)^{\lambda/\rho} + o\left(\varepsilon^{\lambda/\rho}\right)\right]. \tag{45}$$

Proof. Put

$$t_0 = (K/\varepsilon)^{1/\rho}$$

and write $T_{\varepsilon} = t_0(1 + \eta_{\varepsilon})$. The leading equivalence implies $\eta_{\varepsilon} \to 0$. Indeed, for every $\delta \in (0, 1)$, the leading relation in (44) gives

$$u\{t_0(1-\delta)\} > \varepsilon \quad \text{and} \quad u\{t_0(1+\delta)\} < \varepsilon$$

once ε is small enough. Monotonicity then places T_{ε}/t_0 between $1 - \delta$ and $1 + \delta$. Continuity gives $u(T_{\varepsilon}) = \varepsilon$, including when the level set contains an interval. Substitution into $u(T_{\varepsilon}) = \varepsilon$ gives

$$1 = (1 + \eta_{\varepsilon})^{-\rho}\{1 + Dt_0^{-\lambda}(1 + \eta_{\varepsilon})^{-\lambda} + o(t_0^{-\lambda})\}.$$

The remainder is uniform along this sequence because $T_{\varepsilon}/t_0 \to 1$. Rearranging the last display and using the mean-value theorem on $x \mapsto x^{-\rho}$ first yields

$$|\eta_{\varepsilon}| \leq C\{t_0^{-\lambda} + o(t_0^{-\lambda})\},$$

so $\eta_{\varepsilon} = O(t_0^{-\lambda})$. Taylor expansion can therefore be made at the correct scale and gives

$$-\rho\eta_{\varepsilon} + Dt_0^{-\lambda} = o(t_0^{-\lambda}).$$

Since $t_0^{-\lambda} = (\varepsilon/K)^{\lambda/\rho}$, Formula (45) follows. □

The same conclusion follows by two-sided squeezing if u is not strictly decreasing. For every fixed $\eta > 0$, the expansion (44) places the crossing between the two multiplicative trial times obtained by replacing the predicted correction with $D/\rho \pm \eta$. Letting $\eta \downarrow 0$ gives (45).

Monotonicity is a natural sufficient hypothesis for identifying the first threshold crossing with the asymptotic inverse and is available in the application. It is not asserted to be necessary: under alternative global tail-uniform hypotheses, a two-sided squeeze may also control the first crossing. The theorem records the transparent condition used here rather than claiming a minimal inversion principle.

For $0 < \sigma < 1$, use

$$\lambda = \rho\sigma, \qquad D = -\frac{aK^{\sigma}}{\beta}.$$

For $\sigma = 1$, use

$$\lambda = \rho, \qquad D = \frac{M_{\alpha,\beta} - aK}{\beta}.$$

For $\sigma > 1$, use

$$\lambda = \rho, \qquad D = \frac{M_{\alpha,\beta}}{\beta}.$$

Thus the hitting-time correction inherits both the constitutive-memory trichotomy and the exact-power sign transition. When $D_{\alpha,\beta} < 0$, the corrected threshold time is smaller than its leading estimate. When $D_{\alpha,\beta} > 0$, it is larger. At the critical surface the displayed correction vanishes, and (45) supplies no unsupported next rate.

For the exact-power problem, the relative hitting-time coefficient is $D_{\alpha,\beta}/\rho$. Since $\rho = \alpha/\beta$, its magnitude is

$$\frac{|D_{\alpha,\beta}|}{\rho} = \frac{K\Gamma(1-\alpha)\Gamma(1-\rho)}{\alpha u_0 |\Gamma(1-\alpha-\rho)|}.$$

This form is useful for numerical checks because it avoids dividing two separately small fitted quantities.

7. Implicit L1 Discretization and Reproducibility

7.1. Scheme and Nonlinear Step

Let $t_n = nh$ on a uniform grid. The L1 approximation is

$$\delta_h^\alpha U^n = \frac{h^{-\alpha}}{\Gamma(2-\alpha)} \sum_{k=0}^{n-1} a_k (U^{n-k} - U^{n-k-1}), \tag{46}$$

where

$$a_k = (k+1)^{1-\alpha} - k^{1-\alpha}.$$

The L1 method has an extensive convergence and error-analysis literature [14], while complete-monotonicity-preserving schemes have a qualitative structure theory covering stability, comparison, and monotonicity preservation [15]. Long-time rate preservation has also been analyzed for nonlinear fractional ordinary and evolution equations [16,17]. The present calculation asks a different question: whether a computed solution resolves the derived second coefficient over accessible time windows.

Collecting the known history terms in (46) gives

$$\kappa_\alpha U^n + \phi(U^n) = \kappa_\alpha H_n, \qquad \kappa_\alpha = \frac{h^{-\alpha}}{\Gamma(2-\alpha)}, \tag{47}$$

where

$$H_n = a_{n-1} U^0 + \sum_{j=1}^{n-1} (a_{n-j-1} - a_{n-j}) U^j. \tag{48}$$

All coefficients in (48) are positive and sum to one. For the restoring laws used in the computations, ϕ extends continuously to $[0, u_0]$, $\phi(0) = 0$, and ϕ is strictly increasing on that interval. Hence, if $H_n > 0$, the left side of (47) is strictly increasing, negative relative to the right side at $U = 0$, and positive at $U = H_n$. Each computed step therefore has exactly one root in $(0, H_n)$.

For completeness, positivity follows from the strict decrease of a_k. That decrease is a consequence of concavity of $x \mapsto x^{1-\alpha}$. The coefficient sum telescopes:

$$a_{n-1} + \sum_{j=1}^{n-1} (a_{n-j-1} - a_{n-j}) = a_0 = 1.$$

Consequently H_n is a convex combination of the previously computed values. This identity is also an implementation check: a history value outside their closed range signals an indexing or roundoff error before the nonlinear solve is attempted.

The reproducibility script solves (47) by a safeguarded Newton iteration. Newton steps that leave the bracket are replaced by bisection. Every accepted step is checked for a scale-normalized nonlinear residual, positivity, and monotonicity. No random input is used. Direct history summation costs $O(N^2)$. This is adequate for verification runs and avoids introducing a fast-memory approximation whose error would require a second audit.

The L1 formula is used for transparency and qualitative stability. It is not the most efficient long-time method. Sum-of-exponentials and other fast convolution techniques would reduce the cost, but their kernel-compression error could occur at the scale of the second coefficient being measured. Direct summation instead leaves every numerical control explicit: the step size, terminal time, nonlinear target tolerance, 80-iteration cap, fallback residual threshold, and monotonicity-check tolerance. Algorithm 1 states the accepted step together with these safeguards.

Algorithm 1. Safeguarded scalar L1 step.

Step 1: Precompute a_k, their positive backward differences, and κ_α.
Step 2: At time index n, evaluate H_n from the accepted values.
Step 3: Initialize the bracket $[0, H_n]$ and clip U^{n-1} to it for the first trial.
Step 4: Evaluate

$$F_n(x) = \kappa_\alpha(x - H_n) + \phi(x)$$

and its derivative. Accept a Newton trial only when it lies strictly inside the bracket.
Step 5: Otherwise, bisect and stop when

$$|F_n(x)| \leq 2 \times 10^{-14} \max\{1, \kappa_\alpha H_n\}.$$

At most 80 safeguarded iterations are taken. If the target is not reached, reject the run whenever the final scaled residual exceeds 2×10^{-13}.
Step 6: Reject any run containing a non-finite or nonpositive value, or a positive increment exceeding 2×10^{-12}.

The bracket proves existence and uniqueness of each discrete nonlinear solve. The post-run monotonicity assertion tests the computed sequence. It is not silently promoted to a theorem about the continuous derivative.

7.2. Residual Observables

For the exact-power model define

$$R_q(t_n) = t_n^\rho \left[\frac{\Gamma(1-\alpha) t_n^\alpha c (U^n)^\beta}{u_0} - 1 \right] \tag{49}$$

and

$$R_u(t_n) = t_n^\rho \left[\frac{U^n t_n^\rho}{K} - 1 \right]. \tag{50}$$

The continuous theorem predicts

$$R_q(t_n) \to M_{\alpha,\beta}, \qquad R_u(t_n) \to D_{\alpha,\beta}, \tag{51}$$

provided discretization error is negligible on the selected asymptotic window. For $\sigma < 1$, the state residual is instead multiplied by $t_n^{\rho\sigma}$. The theoretical constants are evaluated directly from (30), (32), and (36) inside the script.

Two limits are kept separate. Fixed-terminal-time runs with decreasing h diagnose mesh dependence. Long-time runs at one fixed fine step diagnose approach to the asymptotic coefficient. Changing T and h together would confound these errors and is not used to claim a convergence order.

For a hitting-time diagnostic, a threshold crossing can be interpolated between the first two grid values that straddle it. The leading and corrected predictions are then evaluated from (30), (36), and (45). Such an interpolation is useful for comparing the two asymptotic formulas, but it is not an independent estimate of the time-discretization order.

7.3. Parameter Sets

Table 1 lists the deterministic parameter matrix, which contains six cases with $c = u_0 = 1$.

Table 1. Parameter sets for the deterministic numerical experiments.

Case	α	β	σ	a	Purpose
subcritical exact	0.4	2.0	2.0	0	negative memory correction
critical exact	0.6	1.5	2.0	0	cancellation at $\alpha + \rho = 1$
supercritical exact	0.8	2.0	2.0	0	positive memory correction
constitutive	0.6	2.0	0.5	0.5	constitutive dominance
resonant	0.6	2.0	1.0	0.5	equal correction scales
memory	0.6	2.0	2.0	0.5	memory dominance

The long-time grid uses $h = 0.5$ and $T = 3000$. A separate exact-power mesh study uses

$$(\alpha, \beta, c, u_0) = (0.6, 2, 1, 1), \qquad T = 256, \qquad h \in \{1, 0.5, 0.25, 0.125\}.$$

These choices test signs and scale separation. They do not certify endpoint regularity.

The first three rows straddle the analytic surface $\alpha + \alpha/\beta = 1$: their values are 0.6, 1, and 1.2. The last three rows fix $\rho = 0.3$. Their constitutive exponents $\rho\sigma$ are 0.15, 0.3, and 0.6, while the memory exponent remains 0.3. The matrix therefore changes one mechanism at a time and tests both sides of each trichotomy without fitting a threshold from the computed data.

The choice $T = 3000$ is a pragmatic diagnostic horizon, not a theorem about the onset of the asymptotic regime. With $h = 0.5$, it gives $N = 6000$ steps and about 1.8×10^7 direct history interactions, while retaining four equally spaced checkpoints at $750, 1500, 2250, 3000$. Across those checkpoints, both exact-power noncritical estimators move monotonically toward their predicted coefficients, and the critical estimator decreases in magnitude from 0.003312 to 0.001446. The terminal relative discrepancies range from below 1% in the subcritical and resonant cases to about 14% in the slowest memory-dominant case. Thus $T = 3000$ is sufficient to resolve the predicted signs and scale competition in these runs, but it is not claimed to place every case in a high-accuracy asymptotic regime. The full window trends and the separate fixed-T mesh study are reported precisely to expose this remaining finite-horizon bias.

8. Numerical Diagnostics

This section reports the diagnostics produced by the scheme of Section 7 for the six parameter sets of Table 1. Table 2 collects the principal outcomes, and the three subsections that follow examine the exact-power threshold, the constitutive–memory competition, and the mesh and solver checks in turn.

Table 2. Summary of the principal numerical diagnostics. Relative discrepancies compare the terminal scaled estimator with the nonzero predicted coefficient.

Case	**Prediction**	**Diagnostic at $T = 3000$**	**Main Finding**
exact, subcritical	-0.320252	-0.317534	negative sign; 0.85% discrepancy
exact, critical	0	-0.001446	magnitude falls by 56% from $t = 750$
exact, supercritical	0.274068	0.286782	positive sign; 4.6% discrepancy
constitutive, $\sigma = 0.5$	-0.204853	-0.212347	slower constitutive scale is observed first
resonant, $\sigma = 1$	-0.269465	-0.267142	combined coefficient; 0.86% discrepancy
memory, $\sigma = 2$	-0.101606	-0.116007	correct sign, with the largest finite-window gap

8.1. Exact-Power Threshold

The computed coefficient estimators reproduce the sign transition. Table 3 reports the terminal values at $T = 3000$.

Table 3. Exact-power state-coefficient diagnostics at $T = 3000$.

Regime	**Predicted $D_{\alpha,\beta}$**	**Computed $R_u(T)$**	**State Ratio $U(T)T^{\rho}/K$**
subcritical	-0.320252	-0.317534	0.935973
critical	0	-0.001446	0.999941
supercritical	0.274068	0.286782	1.011660

The subcritical estimate differs from the prediction by about 0.85% at the terminal time. The critical estimator decreases in magnitude from -0.003312 at $t = 750$ to -0.001446 at $t = 3000$, consistent with cancellation of the displayed $t^{-\rho}$ term. No next exponent is fitted. The supercritical value approaches the positive coefficient from above and retains a visible finite-window bias, which is reported rather than removed by selective truncation.

The four-window sequences make the direction of convergence transparent. For the subcritical run, $R_u(t)$ takes the values

$$-0.316430, \quad -0.317042, \quad -0.317342, \quad -0.317534$$

at $t = 750, 1500, 2250, 3000$, respectively. The corresponding supercritical values are

$$0.295732, \quad 0.290686, \quad 0.288280, \quad 0.286782.$$

Thus neither agreement in Table 3 results from choosing a single favorable endpoint. Both sequences move steadily toward the analytic coefficient, although the supercritical error at $T = 3000$ is still about 4.6%. These monotone window trends are useful diagnostics, but they are not used as proofs of convergence.

The dissipation ratio converges more slowly in the subcritical example. At $T = 3000$,

$$\frac{\Gamma(1-\alpha)T^{\alpha}cU(T)^{\beta}}{u_0} = 0.876045.$$

This does not contradict the state-coefficient agreement. The two normalizations have different finite-time biases, and the low fractional order gives a slow leading-ratio approach.

8.2. Constitutive-Memory Competition

Table 4 uses the scale prescribed by Theorem 3.

The resonant case is already within one percent of its predicted combined coefficient. The constitutive-dominant estimator approaches its limit from below in magnitude. The memory-dominant example has the largest residual gap at the chosen terminal time. These are empirical finite-window observations; the little-o remainder in Theorem 3 determines neither the direction nor the monotonicity of approach.

Table 4. Constitutive-memory coefficient diagnostics at $T = 3000$.

Regime	Predicted First State Coefficient	Computed Scaled Coefficient at $T = 3000$
$\sigma = 0.5$	−0.204853	−0.212347
$\sigma = 1$	−0.269465	−0.267142
$\sigma = 2$	−0.101606	−0.116007

The full window data distinguish the three behaviors more clearly. For $\sigma = 0.5$, the scaled coefficient changes from -0.214744 to -0.212347, moving toward -0.204853. At resonance it changes from -0.265687 to -0.267142, moving toward the combined coefficient -0.269465. For $\sigma = 2$, it changes from -0.123825 to -0.116007, moving toward -0.101606 over the observed windows but with a larger residual gap. The three finite-window sequences move toward their predicted coefficients. No claim about the sign or structure of an omitted term is made, because Theorem 3 specifies only a little-o remainder.

8.3. Mesh and Solver Checks

At fixed $T = 256$, the exact-power state value changes from 0.12461056 for $h = 1$ to 0.12454297 for $h = 0.125$. The scaled state-correction estimator changes from -0.107976 to -0.110780. The movement is small relative to the difference between the finite-T estimator and the asymptotic value -0.101606. Thus asymptotic truncation, not mesh variation over these four grids, is the dominant visible error at this terminal time.

Successive changes in the terminal state are 3.8790×10^{-5}, 1.9252×10^{-5}, and 9.5515×10^{-6}. Their near-halving is consistent with first-order refinement on this fixed terminal interval. The analogous changes in the scaled coefficient are 1.6094×10^{-3}, 7.9876×10^{-4}, and 3.9629×10^{-4}. These observations are a resolution check, not a convergence-rate theorem: the weak initial singularity and the growing-memory horizon require a separate error analysis. In particular, validation of the continuous second coefficient would require an estimate such as $T^{2\rho}|U^N - u(T)| = o(1)$ in a controlled joint $T \to \infty$, $h \to 0$ regime; no such estimate is proved here.

Across all six long-time runs, the largest scale-normalized nonlinear residual was below 2.0×10^{-14}. Every stored value was finite and positive, and the largest positive increment was zero to the stated 2×10^{-12} tolerance. These checks validate the discrete calculation. They do not prove continuous ultimate convexity or the endpoint hypothesis.

The source file `draft_numerics.py`, the three CSV files, and the runtime manifest reproduce every value in this section. These files are available from the author on request. The reported tables are cross-checked against the corresponding CSV fields; the script does not itself typeset the Markdown tables.

The archived run manifest records Python 3.12.13 and NumPy 2.3.5 as the generation environment. Re-running the script requires a compatible Python environment with NumPy installed. The accompanying checksum ledger records the full SHA-256 value of the script and every generated data file.

Reported decimals are intentionally fewer than the solver output provides. They indicate the scale resolved by the experiment and avoid presenting floating-point precision as asymptotic accuracy. The script stores the full values so that rounding, table construction, and any later plotting remain auditable.

9. Discussion, Limitations, and Open Problems

The second term in a finite-mass Caputo convolution is controlled by more than the tail ratio of the state. Formula (2) shows the reason directly. The leading term sees the total dissipated mass u_0. The next term sees how the remaining Stieltjes mass is distributed over the whole interval, including a singular terminal layer. Ordinary regular variation gives the correct interior scaling but cannot exclude terminal concentration.

The counterexample distinguishes this result from a routine application of a fractional Karamata formula. It changes the function by a vanishing relative amount, keeps positivity, decrease, local absolute continuity, and regular variation, yet makes the normalized convolution residual diverge. The endpoint condition is therefore tied to the operator, not to a preference for smooth trajectories.

Operator-level regular-variation results remain central prior art. Řehák provides a systematic treatment of fractional operators and regular variation [8] and studies fractional differentiation of asymptotic relations [7]. The present theorem addresses a decreasing finite-mass tail of negative index, retains the initial-value contribution, and isolates the terminal singularity through (5). Its contribution is the combination of that endpoint criterion with a construction showing failure under bare $RV_{-\rho}$; the beta–gamma quotient itself belongs to the established operator theory.

The nonlinear equation has two independent sources of finite-time bias. The Caputo derivative carries a memory correction at relative order $t^{-\rho}$. The restoring law carries a local perturbation at relative order $t^{-\rho\sigma}$. Their exponents, rather than an informal division between "global" and "local" effects, determine which coefficient is observable first.

The resonant case $\sigma = 1$ is especially sensitive. Memory and constitutive coefficients add at one scale, and parameters may make their sum small. A small combined coefficient does not improve the remainder automatically. It exposes terms that the assumed expansion of ϕ does not specify. The exact-power critical surface has the same caution. It proves that the displayed memory term vanishes, not that a universal third term exists.

The hitting-time formula gives both finite-time biases an operational meaning. Let $T_\varepsilon^{(0)} = (K/\varepsilon)^{1/\rho}$ be the leading threshold estimate. Equation (45) shows that its signed relative correction is $(D/\rho)(\varepsilon/K)^{\lambda/\rho}$. Hence $D < 0$ means that the state lies below its leading profile and reaches the threshold earlier than $T_\varepsilon^{(0)}$; $D > 0$ means a later crossing. For $\sigma < 1$, this sign is controlled by the constitutive coefficient $-aK^\sigma/\beta$. At resonance it is controlled by the combined coefficient $(M_{\alpha,\beta} - aK)/\beta$, so the two mechanisms can reinforce or offset each other. For $\sigma > 1$, the memory coefficient $M_{\alpha,\beta}/\beta$ controls the sign. In the exact-power model this changes at $\alpha = \beta/(\beta + 1)$, converting the analytic sign transition into a reversal of the leading hitting-time forecast bias.

The main limitation is the endpoint hypothesis. Propositions 1 and 2 make it usable, but they do not prove it for every trajectory of (24). Automatic ultimate convexity for the exact-power equation remains open. The Volterra Equation (43) suggests one route, but positivity of its solution is not enough to establish decrease of $y = -u'$.

The general restoring-law theorem identifies only the first correction. When $\sigma < 1$, a longer constitutive expansion can generate several powers before the memory scale. At the global critical surface or a resonant coefficient cancellation, the next nonzero term likewise requires additional operator and constitutive information.

The computations cover representative scalar parameters on uniform grids. They do not study nonuniform meshes, fast-memory approximations, systems, variable order, delay, or partial differential equations. Numerical agreement is evidence that the formulas and implementation are mutually consistent, not evidence for an analytic hypothesis.

These limitations separate two different questions. Internally, the endpoint Abelian theorem is complete under its stated uniform-integrability hypothesis, and the counterexample proves that some endpoint control is necessary. Externally, applying the theorem to every solution of a particular fractional equation requires an independent route to that hypothesis. The current paper supplies two sufficient routes and keeps the unresolved route explicit. This distinction prevents a conditional application statement from being mistaken for a gap in the operator theorem itself.

The first open problem is to prove or disprove automatic endpoint regularity for broad classes of autonomous nonlinear Caputo relaxation trajectories. A second is to derive the first nonzero term on $\alpha + \alpha/\beta = 1$. A third is to formulate a multicomponent analogue in which the scalar memory coefficients interact through an exponent matrix. Discrete second-order asymptotics also deserve separate analysis: a long-time L1 solution contains both physical and numerical memory corrections, and their separation is not supplied by continuous theory alone.

For systems, a scalar replacement of β is unlikely to be sufficient. Different components may decay with different regularly varying indices, so the second memory vector can couple endpoint masses with the Jacobian of the restoring map. A viable extension should first identify a positive invariant cone and then formulate endpoint uniform integrability componentwise or in a weighted norm. Only after that operator step would a matrix-valued analogue of the constitutive-memory trichotomy be justified.

10. Conclusions

For a decreasing finite-mass tail, first-order regular variation does not determine the second Caputo term. The missing information lies at the singular terminal endpoint. Under (5), the exact Stieltjes decomposition and the three-region limit give the beta–gamma coefficient; the plateau–catch-up example shows why additional terminal control cannot be discarded over the full $RV_{-\rho}$ class.

The nonlinear conclusions inherit this conditional scope. For $\phi(x) = cx^{\beta}\{1+ax^{\sigma}+o(x^{\sigma})\}$, asymptotic inversion separates constitutive dominance, resonance, and memory dominance according as $\sigma < 1$, $\sigma = 1$, or $\sigma > 1$. In the exact-power case, the first relative coefficient changes sign at $\alpha = \beta/(\beta+1)$ and vanishes at equality. The same coefficient corrects residual hitting times. The L1 calculations are consistent with these signs and scales, while leaving the continuous endpoint hypothesis and the discrete second-order error as separate analytical questions.

Four directions now have concrete prerequisites. First, automatic endpoint regularity for broad autonomous trajectories requires a Volterra comparison or resolvent argument that proves eventual decrease of $y = -u'$, not merely positivity. Second, a nonzero term on the critical surface requires a rate version of the endpoint Abelian theorem together with a longer constitutive expansion. Third, a joint $T \to \infty$, $h \to 0$ error theory is needed to separate physical and discrete memory corrections and to assess fast-memory schemes at the second-coefficient scale. Fourth, vector extensions require an invariant cone and a componentwise or weighted-norm endpoint condition before matrix-valued asymptotic inversion is attempted. Each direction therefore demands information beyond the first-order tail used here.

Funding

This research received no external funding.

Institutional Review Board Statement

Not applicable.

Informed Consent Statement

Not applicable.

Data Availability Statement

The code and data supporting this study are available from the author on request. They comprise the reproducibility script `draft_numerics.py`, the three generated CSV files, the runtime manifest, and the SHA-256 checksum ledger. The numerical calculations are deterministic and use no external or third-party dataset.

Conflicts of Interest

The author declares no conflict of interest.

Use of AI and AI-Assisted Technologies

No AI tools were utilized for this paper.

References

1. Feng, Y.; Li, L.; Liu, J.G.; et al. Continuous and Discrete One Dimensional Autonomous Fractional ODEs. *Discret. Contin. Dyn. Syst. B* **2018**, *23*, 3109–3135. https://doi.org/10.3934/dcdsb.2017210.
2. Li, L.; Liu, J.G. A Generalized Definition of Caputo Derivatives and Its Application to Fractional ODEs. *SIAM J. Math. Anal.* **2018**, *50*, 2867–2900. https://doi.org/10.1137/17m1160318.
3. Furati, K.M.; Tatar, N.E. Power-Type Estimates for a Nonlinear Fractional Differential Equation. *Nonlinear Anal. Theory Methods Appl.* **2005**, *62*, 1025–1036. https://doi.org/10.1016/j.na.2005.04.010.
4. Furati, K.M.; Tatar, N.E. Long Time Behavior for a Nonlinear Fractional Model. *J. Math. Anal. Appl.* **2007**, *332*, 441–454. https://doi.org/10.1016/j.jmaa.2006.10.027.
5. Vergara, V.; Zacher, R. Optimal Decay Estimates for Time-Fractional and Other NonLocal Subdiffusion Equations via Energy Methods. *SIAM J. Math. Anal.* **2015**, *47*, 210–239. https://doi.org/10.1137/130941900.
6. Bingham, N.H.; Goldie, C.M.; Teugels, J.L. *Regular Variation*; Cambridge University Press: Cambridge, UK, 1987. https://doi.org/10.1017/cbo9780511721434.
7. Řehák, P. Fractional Integration and Differentiation of Asymptotic Relations and Applications. *Math. Methods Appl. Sci.* **2025**, *48*, 6381–6395. https://doi.org/10.1002/mma.10679.

8. Řehák, P. Regular Variation and Fractional Operators. *Fract. Calc. Appl. Anal.* **2026**, *29*, 662–682. https://doi.org/10.1007/s13540-026-00501-0.
9. de Haan, L.; Stadtmüller, U. Generalized Regular Variation of Second Order. *J. Aust. Math. Soc.* **1996**, *61*, 381–395. https://doi.org/10.1017/s144678870000046x.
10. Mao, T.; Hua, L. Second-Order Regular Variation Inherited from Laplace–Stieltjes Transforms. *Commun. Stat. Theory Methods* **2016**, *45*, 4569–4588. https://doi.org/10.1080/03610926.2014.922990.
11. Diethelm, K. *The Analysis of Fractional Differential Equations: An Application-Oriented Exposition Using Differential Operators of Caputo Type*; Springer: Berlin/Heidelberg, Germany, 2010. https://doi.org/10.1007/978-3-642-14574-2.
12. Clément, P.; Nohel, J.A. Asymptotic Behavior of Solutions of Nonlinear Volterra Equations with Completely Positive Kernels. *SIAM J. Math. Anal.* **1981**, *12*, 514–535. https://doi.org/10.1137/0512045.
13. Prüss, J. *Evolutionary Integral Equations and Applications*; Birkhäuser: Basel, Switzerland, 1993. https://doi.org/10.1007/978-3-0348-8570-6.
14. Stynes, M. A Survey of the L1 Scheme in the Discretisation of Time-Fractional Problems. *Numer. Math. Theory Methods Appl.* **2022**, *15*, 1173–1192. https://doi.org/10.4208/nmtma.oa-2022-0009s.
15. Li, L.; Wang, D. Complete Monotonicity-Preserving Numerical Methods for Time Fractional ODEs. *Commun. Math. Sci.* **2021**, *19*, 1301–1336. https://doi.org/10.4310/cms.2021.v19.n5.a6.
16. Wang, D.; Xiao, A.; Zou, J. Long-Time Behavior of Numerical Solutions to Nonlinear Fractional ODEs. *ESAIM Math. Model. Numer. Anal.* **2020**, *54*, 335–358. https://doi.org/10.1051/m2an/2019055.
17. Wang, D.; Stynes, M. Optimal Long-Time Decay Rate of Numerical Solutions for Nonlinear Time-Fractional Evolutionary Equations. *SIAM J. Numer. Anal.* **2023**, *61*, 2011–2034. https://doi.org/10.1137/22m1494361.